Germ-line elimination of electric charge on pre-T-cell receptor (TCR) impairs autonomous signaling for β-selection and TCR repertoire formation

Ishikawa, Eri
Division of Molecular Immunology, Research Center for Infectious Diseases, Medical Institute of Bioregulation, Kyushu University

Miyake, Yasunobu
Division of Molecular Immunology, Research Center for Infectious Diseases, Medical Institute of Bioregulation, Kyushu University

Hara, Hiromitsu
Department of Biomolecular Sciences, Faculty of Medicine, Saga University

Saito, Takashi
World Premier International Immunology Frontier Research Center, Osaka University

他

出版情報：Proceedings of the National Academy of Sciences of the United States of America. 107 (46), pp.19979-19984, 2010-11-16. National Academy of Sciences
バージョン：

Biological Science / Immunology

Germline elimination of electric charge on pre-TCR impairs autonomous signaling for β-selection and TCR repertoire formation

Eri Ishikawa[*], Yasunobu Miyake[*], Hiromitsu Hara[†], Takashi Saito[§,¶] and Sho Yamasaki[*,§]

[*]Division of Molecular Immunology, Research Center for Infectious Diseases, Medical Institute of Bioregulation, Kyushu University, 3-1-1, Maidashi, Fukuoka, 812-8582, Japan.

[†]Department of Biomolecular Sciences, Faculty of Medicine, Saga University, 5-1-1 Nabeshima, Saga 849-8501, Japan.

[§]Laboratory for Cell Signaling, RIKEN Research Center for Allergy and Immunology, 1-7-22 Suehiro-cho, Tsurumi-ku, Yokohama 230-0045, Japan

[¶]World Premier International Immunology Frontier Research Center, Osaka University, 1-1, Yamadaoka, Suita, 565-0871, Japan.

Correspondence to: Sho Yamasaki
Division of Molecular Immunology, Medical Institute of Bioregulation,
Kyushu University, 3-1-1 Maidashi, Higashiku, Fukuoka, 812-8582, Japan.
Phone/FAX: +81-92-642-4614
e-mail: yamasaki@bioreg.kyushu-u.ac.jp

Abstract

The pre-T cell receptor (pre-TCR) is crucial for the early T cell development, but the ligand for pre-TCR remains unidentified. We recently proposed a model that pre-TCR complexes oligomerize spontaneously through interactions of the pre-TCRα chain. To investigate the mechanism underlying this ligand-independent signaling *in vivo*, we established knock-in mice that express a pre-TCRα mutant lacking charged amino acids ($D^{22}R^{24}R^{102}R^{117}$ to $A^{22}A^{24}A^{102}A^{117}$; 4A). $CD4^+CD8^+$ thymocyte number was significantly reduced in $pT\alpha^{4A/4A}$ mice, whereas $CD4^-CD8^-$ thymocytes were unaffected. The percentages of DN3 cells and γδ T cells were increased in the $pT\alpha^{4A/4A}$ thymus, indicating that β-selection is impaired in $pT\alpha^{4A/4A}$ mice. Pre-TCR-mediated tyrosine phosphorylation and clonal expansion into DP thymocytes were also defective in the knock-in mice. Pre-TCR was expressed at higher levels on $pT\alpha^{4A/4A}$ cell surfaces than on those of the wild-type, suggesting that the charged residues in pTα are critical for autonomous engagement and subsequent internalization of pre-TCR. Pre-TCR-mediated allelic exclusion of the TCRβ gene was also inhibited in $pT\alpha^{4A/4A}$ mice, and thereby dual TCRβ were expressed on $pT\alpha^{4A/4A}$ T cells. Furthermore, the TCRVβ repertoire of mature T cells was significantly altered in $pT\alpha^{4A/4A}$ mice. These results suggest that charged residues of pTα are critical for β-selection, allelic exclusion, and TCRβ repertoire formation.

\body

Introduction

The pre-T cell receptor (pre-TCR) is a multimeric complex consisting of variable rearranged TCRβ chains, an invariant pre-TCRα (pTα) chain, and CD3 molecules. Pre-TCR is crucial for T cell development from the $CD4^{-}CD8^{-}$ (double-negative; DN) to the $CD4^{+}CD8^{+}$ (double-positive; DP) stages, a process known as β-selection. Despite its structural similarity to mature αβTCR, which requires MHC-antigen for engagement, it has been proposed that pre-TCR initiates signals in a ligand-independent manner (1, 2). Several mechanisms have been proposed in attempts to explain how pre-TCR mediates autonomous signaling (3-6); however, the precise molecular mechanism underlying the process remains unclear (2).

We have recently proposed that the pre-TCR complex forms oligomers spontaneously. The pTα–erythropoietin receptor (EPOR) chimera indeed triggers a growth signal autonomously through self-oligomerization and four conserved charged residues (D22, R24, R102, and R117) are critical for the functioning of pTα–EPOR (7).

Part of the difficulty in analyzing the pre-TCR signal *in vivo* arises because the threshold for the β-selection checkpoint is quite low and thus a very precise dosage of the expressed pre-TCR needs to be achieved. One reason for this low threshold is that the DN stage is uniquely sensitive to signals mediated by the immunoreceptor tyrosine-based activation motif (ITAM) (7-10). The high sensitivity of DN cells may arise from a) the co-expression of Syk and ZAP-70 in the DN stage (10); b) the high level of expression of micro-RNA (mir181a) in the DN stage, which enhances T cell responsiveness by

suppressing several inhibitory phosphatases (11); c) the predominant role of Rap1 rather than Ras downstream of pre-TCR (12); or d) the expression of CXCR4 as a costimulatory receptor of pre-TCR (13, 14). Therefore, the overexpression of pTα mutants might overcome their original structural requirements. Indeed, although many studies have addressed mutagenesis analysis of pTα by using transgenic- or retroviral-introduction of mutant pTα, conclusions regarding the definitive functional domain remain a matter of controversy (3-9, 15, 16). These observations suggest that the structure–function relationship of pTα needs to be analyzed with the pTα mutant present at the correct times, amounts, and locations.

Pre-TCR-mediated signaling inhibits further rearrangement of TCRβ chain, which is called allelic exclusion (17). Since pre-TCR signal is triggered autonomously and independent of individual TCRβ chain, pre-TCR may also contribute to generate a diversity of TCRβ during β-selection. Therefore optimal pre-TCR signal might play a crucial role in shaping appropriate TCRβ repertoire in mature T cells. However, this issue has not been clearly addressed, as $pT\alpha^{-/-}$ mice shows severe defect in the development of mature T cells themselves (18).

In the current study, to fulfill those prerequisites, we employed a knock-in approach and demonstrated that charged residues in pTα are critical for the initiation of the pre-TCR signal, β-selection, and TCRβ repertoire formation.

Results

Generation of knock-in mice expressing "charge-less" pTα chain

To examine whether the charged residues are crucial for pre-TCR-mediated β-selection *in vivo*, we generated knock-in mice that expressed a pTα mutant in which four residues (D22, R24, R102 and R117) were exchanged for alanine, a neutral residue (Fig. 1A). A targeting construct bearing four point mutations in two exons was used for homologous recombination, and the *Neo* cassette was deleted after germline transmission (Fig. 1B). The knock-in allele was detected by means of primers located on both sides of *loxP* sites (Fig. 1C). Homozygous $pT\alpha^{4A/4A}$ mice were born at rates consistent with Mendelian inheritance and they showed no obvious abnormalities.

First, we analyzed whether the mutant allele was normally expressed by comparing mRNA levels for $pT\alpha^{WT}$ and $pT\alpha^{4A}$ in DN thymocytes from WT ($pT\alpha^{+/+}$), heterozygous knock-in ($pT\alpha^{4A/+}$), homozygous knock-in ($pT\alpha^{4A/4A}$) and knock out ($pT\alpha^{-/-}$) mice. We designed common primers for both pTα alleles as well as specific primers that were able to distinguish between the WT and mutant allele, and we confirmed that the total amount of pTα was constant and that mutant pTα was properly expressed from the targeted allele (Fig. 1D).

Next, we confirmed the expression of $pT\alpha^{4A}$ proteins (Fig. 1E). Pre-TCR was shown to be expressed at very low levels on the surface of WT thymocytes, as the degree of specific staining of anti-pTα or anti-TCRβ was only slightly higher than those of isotype control antibodies (7, 19). This slight shift was significant because it was absent in $pT\alpha^{-/-}$ thymocytes. However, surface pre-TCR was clearly detected on $pT\alpha^{4A/4A}$

thymocytes (Fig. 1E), indicating that the mutant pTα protein was correctly expressed and thus likely assembled with the other components of the pre-TCR complex.

From these observations, we could confirm that the successful establishment of the knock-in mice expressing "charge-less" pTα.

Impaired thymocyte development in pTα$^{4A/4A}$ mice

We first examined thymic cellularity in pTα$^{4A/4A}$ mice. The total number of thymocytes was significantly reduced in pTα$^{4A/4A}$ mice compared with pTα$^{+/+}$ mice (Fig. 2A). Population analyses revealed that in pTα$^{4A/4A}$ mice, the number of CD4^{+}CD8^{+} (DP) thymocytes, but not that of CD4^{-}CD8^{-} (DN) thymocytes, was reduced, showing that differentiation from DN to DP was blocked by the charge-eliminating mutation of pTα (Fig. 2B). The percentage of DP thymocytes was also decreased in pTα$^{4A/4A}$ mice (Fig. 2C), although the reduction was not as drastic. We therefore conducted a precise examination of the efficiency of β-selection in pTα$^{4A/4A}$ thymocytes using an *in vitro* differentiation system (7). DN thymocytes from WT mice gave rise to over 20% of DP cells when cultured on stroma cells expressing the Notch1 ligand for two days (20, 21). However, the proportion of pTα$^{4A/4A}$-derived DP cells was only one-fifth of that of WT mice, offering further confirmation that these differentiation defects are significant in a cell-intrinsic way (Fig. 2D).

We further examined the subpopulations of thymocytes that are known to be affected by β-selection. DN thymocytes develop through CD44^{+}CD25^{-} (DN1), CD44^{+}CD25^{+} (DN2), CD44^{-}CD25^{+} (DN3), and CD44^{-}CD25^{-} (DN4) stages. Pre-TCR is

expressed mainly at the DN3 stage, and there are several reports of demonstrations that the blocking of pre-TCR signaling results in an accumulation of a DN3 population (22-24). We therefore examined subpopulations of DN cells in pTα$^{4A/4A}$ mice, and found that the DN3 population accumulated significantly in these mice (Fig. 2E).

It has been shown that impairment of pre-TCR signaling also results in an increase in the ratio of γδ T cells, because the pre-TCR signal is critical for the development of αβ T cells but not that of γδ T cells (18). Indeed, the proportions of γδ T cells were significantly increased in pTα$^{4A/4A}$ mice (Fig. 2F). The absolute number of thymic γδ T cells was increased slightly in the pTα$^{4A/4A}$ mice (WT, $1.76 \pm 0.59 \times 10^5$ vs. pTα$^{4A/4A}$, $3.38 \pm 1.62 \times 10^5$). However, these γδ T cells do not account for the phenotypes of αβ T cells in pTα$^{4A/4A}$ mice, since impaired β-selection was observed even in the absence of γδ T cells, i.e. in pTα$^{4A/4A}$ × TCRδ$^{-/-}$ mice (Fig. 2G).

Impaired β-selection in pTα$^{4A/4A}$ mice

Pre-TCR-induced β-selection is also accompanied by robust cell expansion during the DN3 and DN4 stages. We therefore investigated proliferation in these stages by examining the incorporation of 5-bromo-2'-deoxyuridine (BrdU) into thymocytes after injection of the bromonucleoside. Around half the population of DN4 cells was BrdU-positive in WT mice, but this proportion rapidly decreased in DP cells (Fig. 3A, left panels), showing that a massive expansion occurs during the DN3-to-DN4 stages in which pre-TCR expressed. The weak incorporation of BrdU before pre-TCR expression (DN2) was of a similar level in WT and pTα$^{4A/4A}$ mice, but the proportion of

BrdU-positive DN4 cells decreased by half in the pTα$^{4A/4A}$ mice (Fig. 3A, right panels). These results suggest that the pre-TCR-mediated proliferation was still impaired even in the decreased, but still substantial, population of DN4 cells in pTα$^{4A/4A}$ mice.

The impaired β-selection was also reflected in the decreased numbers of peripheral αβ T cells in neonates, although in adult mice this was restored in compensatory manner, so that similar numbers were present to those in WT mice (Fig. S1). The defective ability of mutant T cells to develop was confirmed by means of a competitive repopulation assay in which a 1:1 mixture of BM cells from pTα$^{4A/4A}$ and WT mice was injected into Rag1-deficient recipients. The pTα$^{4A/4A}$-derived BM cells generated a comparable number of DN thymocytes to the WT-derived BM cells. However, the pTα$^{4A/4A}$ DN cells developed into fewer DP, SP and peripheral αβ T cells and equivalent γδ T cells under the competition with WT-derived BM cells (Fig. 3B), confirming that the charged moiety of pTα is critical for optimal development of αβ T cells.

Defective pre-TCR proximal signaling in pTα$^{4A/4A}$ thymocytes

We next analyzed proximal signaling of pre-TCR. Freshly-isolated DN thymocytes from WT mice contained several constitutive phosphorylated proteins (Fig. 3C, lane2). This is highly likely to be mediated by pre-TCR, as it was not detected in pre-TCR-deficient Rag1$^{-/-}$ and pTα$^{-/-}$ thymocytes (Fig. 3C, lanes 1 and 4). Importantly, this pre-TCR-induced phosphorylation of cellular proteins was impaired in pTα$^{4A/4A}$ thymocytes (Fig. 3C, lane 3 and Fig. S2)

Autonomous engagement of pre-TCR also induces constitutive internalization of pre-TCR itself, which leads to low level of surface pre-TCR expression (19). If this low surface expression of pre-TCR is dependent on the charged residues in pTα, surface pre-TCR should be augmented in $pT\alpha^{4A/4A}$ thymocytes. Indeed, surface expression levels of pTα and TCRβ in $pT\alpha^{4A/4A}$ mice were higher than those in WT mice (Fig. 1E, left vs. middle panels).

These results suggest that the proximal events through pre-TCR are dependent on the presence of charge in the pTα chain.

Break of allelic exclusion in $pT\alpha^{4A/4A}$ mice

The pre-TCR signal is critical for extinguishing further rearrangement of the TCRβ chain (17), presumably to avoid producing T cells bearing two different TCRβs on a single cell, a behavior that is called allelic exclusion (25). We therefore examined the effect of pTα mutation on allelic exclusion by introducing transgene of rearranged TCRβ into $pT\alpha^{4A/4A}$ mice as an *in vivo* model of allelic exclusion (26). We confirmed that thymocytes number in $pT\alpha^{4A/4A}$ mice decreased even in the presence of the TCRβ transgene (Fig. S3).

Rearrangement of endogenous *Tcrb* allele was detected by specific primers encompassing TCR Vβs (Vβ5, Vβ8 and Vβ10), TCR Dβ1, and TCR Jβ1 (Fig. 4A). In wild-type DN thymocytes, the products of V-DJ rearrangement was visualized as five major bands reflecting the usage of Jβ1.1, Jβ1.2, Jβ1.3, Jβ1.4 and Jβ1.5, respectively (Fig. 4B, lanes 1-3). D-J rearrangement could also be detected as well by using a Dβ specific

primer (Fig. 4B, lane 1-3). These are specific because no product was detected in $Rag2^{-/-}$ thymocytes, except for germline-derived product (Fig. S4).

The introduction of productive TCRβ transgene (2B4 TCRβ; Vβ3-Jβ2) attenuated V to DJ rearrangement of the endogenous TCRβ chain (Fig. 4B, lanes 4-6). This suppressed V-DJ rearrangement was, however, restored in $pT\alpha^{4A/4A}$ background (Fig. 4B, lanes 10-12). As previously reported, D to J rearrangement was not affected by the transgene (26). The amount of genomic DNA and the genotypes were confirmed by PCR for $TCR\beta^{Tg}$, $pT\alpha^{WT}$ and $pT\alpha^{4A}$ allele (Fig. 4B). These results suggest that the charged residues in pTα are required for the allelic exclusion of TCRβ.

Given that the allelic exclusion of TCRβ was incomplete in $pT\alpha^{4A/4A}$ mice, "single TCR on a single T cell" rule might be also broken in these mice. We therefore examined whether two different TCRβs are expressed on a single T cell in $pT\alpha^{4A/4A}$ mice. To address this possibility, T cells were stained with anti-Vβ3 mAb together with a mixture of all available anti-Vβs mAbs except for Vβ3 ($V\beta_{endo}$). The anti-$V\beta_{endo}$ mixture stained 70% of TCRβ expressed in WT T cells (Fig. 5A, left panels). In TCRβ Tg mice, Tg-derived $V\beta3^{+}$ cells lost the expression of endogenous Vβs as a result of allelic exclusion (Fig. 5A). However, in TCRβ Tg × $pT\alpha^{4A/4A}$ mice, T cell population expressing dual TCRβ on the surface of each cell ($V\beta3^{+}V\beta_{endo}^{+}$) was significantly increased in both SP thymocytes and splenic T cells (Fig. 5A and 5B).

This phenomenon was also observed in non-TCR Tg background, because the frequency of SP thymocytes expressing dual endogenous Vβs increased in $pT\alpha^{4A/4A}$ mice (Fig. 5C, left panel), although this was not observed clearly in splenic T cells at least for

$V\beta3^+$ and $V\beta5^+$ cells (Fig. 5C, right panel).

These results suggest that an optimal pre-TCR signal is critical for preventing the expression of dual TCRβs on a single T cell, which would otherwise lead to autoimmune disorder (27).

TCR repertoire of T cells in $pT\alpha^{4A/4A}$ mice

Autonomous pre-TCR signaling may also contribute to permit diverse TCRβ to pass through β-selection. We finally analyzed whether the repertoire of TCRβ is altered in $pT\alpha^{4A/4A}$ mice by examining the usage of TCRVβ using several mAbs specific for different Vβs. The distribution of TCRVβ was significantly altered in $pT\alpha^{4A/4A}$ SP thymocytes (Fig. 6A) and peripheral T cells (Fig. 6B). Although peripheral T cells were apparently normal in $pT\alpha^{4A/4A}$ mice in terms of number (Fig. S1), alterations in the TCR repertoire might result in defective immune responses of peripheral T cells to a variety of antigens. Further extensive analysis is needed to clarify this issue, since simple allo-reactive T cell responses against B10.D2 ($H\text{-}2^d$) and B10.BR ($H\text{-}2^k$) looked normal in $pT\alpha^{4A/4A}$ T cells.

Taken together, even though pTα is not expressed in mature T cells, the charge on pTα also contributes to shape the subsequent TCR repertoire in the periphery.

Discussion

In this study, we present *in vivo* data supporting the idea that self-engagement of pre-TCR *via* charged residues is significant driving force of β-selection.

The impairment of β-selection in $pT\alpha^{4A/4A}$ mice was significant, but not as severe as that in pTα-deficient mice (Fig. 2A, 2B). This might be because charged residues other than D22, R24, R102, and R117 can compensate for the function of these four residues. Alternatively, the intracellular/transmembrane domain of pTα may have some role in pre-TCR-mediated signaling (15). Interestingly, the proline-rich motif in the pTα tail is proposed to interact with signaling protein(s) thereby facilitating β-selection (5).

It is often argued that substitution of amino acids critical for protein structure may destabilize the protein and thereby impair its function. On the basis of a molecular modeling approach (7), we believe that it does not apply to the four mutations (D22A, R24A, R102A, and R117A) for the following reasons. First, although the substitution of a small residue by bulky residue can sometimes destabilize the structure of a protein, this is not the case for the substitutions by alanine that we used. Secondly, none of these residues is located within a highly fluctuated region, such as a flexible loop, in which a local conformational change occurs; instead, they are located in stable segment within a turn region (D22, R24 and R102) or next to a disulfide bonded cysteine (R117). Thirdly, all these residues are located on the surface of the pTα–TCRβ complex rather than in an internal region of the complex, so that the possibility of substitution changing the folded structure is reduced: indeed, molecular modeling suggests that the $pT\alpha^{WT}$–TCRβ dimer

and the pTα^{4A}–TCRβ dimer are expressed with quite similar conformations (7). Finally, our findings that the surface pre-TCR complex was clearly detected in pTα$^{4A/4A}$ mice by anti-pTα as well as by anti-TCRβ showed that the pTα mutant protein was correctly expressed and thus likely assembled with the other components of the pre-TCR complex (Fig. 1E). The characteristics of pTα^{4A} protein were also confirmed by microscopic and biochemical analyses (Fig. S5).

Initially we assumed that if the charge-mediated interaction of pre-TCR is critical for β-selection, impaired development should be observed to some degree in heterozygous pTα$^{4A/+}$ mice as well, because the quantity of pre-TCR signals would be reduced by pre-TCR^{WT}–pre-TCR^{4A} interactions. There was, however, no significant difference in the total numbers of thymocytes (or any fractions thereof) between WT (pTα$^{+/+}$) and heterozygous (pTα$^{4A/+}$) mice (Fig. 2 and Fig. S1). One possible explanation for this is that even in heterozygous (pTα$^{4A/+}$) mice, pre-TCR^{WT}–pre-TCR^{WT} interactions should still occur, and the probability of this interaction can be stochastically calculated to be one-quarter of that in WT pTα$^{+/+}$ mice. It is therefore possible that the lower but nevertheless substantial frequency of pre-TCR^{WT}–pre-TCR^{WT} interactions could be sufficient to drive β-selection in terms of cell number, particularly in the uniquely sensitive DN context (9). It should be noted that the frequencies of some Vβs were significantly altered even in heterozygous (pTα$^{4A/+}$) mice (Fig. 6), implying that partial reduction of pre-TCR signal might essentially affect β-selection in terms of repertoire formation. The analysis on the dynamics and stoichiometry of the self-engagement of pre-TCR may clarify this issue.

The teleological objective of β-selection would be to generate diverse TCRβ chains that subsequently lead to variety in the αβTCR repertoire. Considering the accumulating evidence for β-selection, pre-TCR may validate the quality of TCRβ by minimum criteria; 1) the capacity to assemble with CD3 and TCRα-like protein, i.e. pTα, and 2) the possession of proper intracellular signaling pathway. This apparently 'permissive' selection may be necessary to secure diversity of TCRβ, but sufficient as a prerequisite selection to confirm productive rearrangement of TCRβ before positive/negative selection, in which the specificity of αβ TCR is strictly verified.

In view of this, it would be tempting to make extensive comparisons of the variety of individual TCRβ sequences in $pT\alpha^{4A/4A}$ and WT thymocytes at the pre-selected DP stages, in order to clarify whether charge-mediated self-oligomerization of pre-TCR indeed contributes to the acquisition of diverse TCRβ chains, which should be critical for the host defense against various foreign antigens. In line with this hypothesis, the frequencies of some particular Vβs were found to significantly decrease in $BrdU^{+}$ proliferating DN4-DP thymocytes (Fig. S6) as well as in the mature T cells (Fig. 6) in $pT\alpha^{4A/4A}$ mice, thus implying that a sufficient strength of pre-TCR signal may therefore be required in order to select diverse Vβ chains during β-selection.

Materials and Methods

Mice. For the generation of pT$\alpha^{4A/4A}$ mice, C57BL/6-derived Bruce4 ES cells (provided by T. Kurosaki, RIKEN) were transfected with a linearized targeting vector. Neomycin-resistant clones were subjected to genomic PCR to identify homologous recombinants. Chimeric mice were bred with C57BL/6 mice to obtain heterozygotes, which were then crossed with CAG-Cre Tg mice (28) with a C57BL/6 background to delete the *Neo* cassette. The pT$\alpha^{-/-}$ mice were provided by H. von Boehmer (Harvard Med. Sch.)(18). 2B4 TCRβ Tg mice were provided by M.M. Davis (Harvard Med. Sch.)(29). TCR$\delta^{-/-}$ mice were provided by S. Itohara by courtesy of Y. Yoshikai (Kyushu Univ.)(30). All mice were maintained in a filtered-air laminar-flow enclosure and given standard laboratory food and water *ad libitum*. Animal protocols were approved by the committee of Ethics on Animal Experiment, Faculty of Medical Sciences, Kyushu University and Research Center for Allergy and Immunology, RIKEN.

Reagents. Anti-pTα (2F5), anti-TCRβ (H57), anti-TCRδ (GL3), mouse IgG_1 (MOPC), anti-BrdU, anti-mouse Vβs and BrdU were obtained from BD Biosciences; anti-CD4 (GK1.5), anti-CD8 (53.6.7), anti-CD25 (TMβ.1), anti-CD44, anti-CD3ε (2C11), and anti-TCRβ (H57) were obtained from eBioscience; and anti-CD4 and anti-CD8 microbeads were obtained from Miltenyi Biotec. Anti-phosphotyrosine (4G10) was from Cell Signaling. Anti-CD3ε was purchased from Santa Cruz Biotechnology.

Flow cytometry. For pre-TCR staining, $CD4^-CD8^-$ DN thymocytes were sorted by

magnetic bead cell sorting (Miltenyi Biotec) and stained with anti-pTα, anti-mIgG-biotin, and streptavidin-APC in the presence of anti-CD4-CyChrome, anti-CD8-CyChrome, anti-CD44-PE, and anti-CD25-FITC. The DN3-to-DN4 transitional population ($CD4^-CD8^-CD44^-CD25^{int}$) was gated and analyzed for surface pTα staining. Control mouse IgG_1 was used as a control mAb for anti-pTα.

In vitro **thymocyte differentiation.** Thymocytes from 4-week-old mice were cultured on Tst4 cells expressing DLL1-IRES-GFP (31). At day 3 of culture, cells were analyzed for CD4 and CD8 expression after gating out of stroma cells by using the forward scatter (FSC) – side scatter (SSC) and fluorescence channel 1 (FL1) gate.

Competitive repopulation assay. 5 x 10^6 BM cells from WT mice and $pT\alpha^{4A/4A}$ mice were mixed at ratio of 1:1 and injected intravenously into irradiated (4Gy) $Rag1^{-/-}$ mice. Reconstituted thymi and spleens were analyzed 4 wk later. Each mixed BM cells were injected at least five recipient mice with sex and age matched.

Real-time PCR. Real-time PCR was performed using the primers as follows:
pan-pTα, 5'- GGGGCTGGGGGACAGAA -3' (forward) 5'- GGGCTCAGAGGGGTGG GTAA -3' (reverse); $pT\alpha^{WT}$, 5'- GGGGAATCTTCGACAGCCAG -3' (forward) 5'- GGG CTCAGAGGGGTGGGTAA -3' (reverse); $pT\alpha^{4A}$, 5'- GGGGAATCTTCGACAGCCGC -3' (forward) 5'- GGGCTCAGAGGGGTGGGTAA -3' (reverse); β-actin, 5'- TGGAATC CTGTGGCATCCATGAAAC -3' (forward) 5'- TAAAACGCAGCTCAGTAACAGTCC

G -3' (reverse).

BrdU incorporation. Mice were injected intraperitoneally with 1 mg BrdU and then sacrificed 4 h later. After surface staining with anti-CD8, anti-CD4, anti-CD25 and anti-CD44, the thymocytes were fixed and permeabilized with Cytofix/Cytoperm buffer followed by treatment with DNase. Cells were stained with APC-conjugated anti-BrdU Ab (BD Biosciences).

Western blot analysis. DN thymocytes were freshly isolated by negative sorting using anti-CD8 and anti-CD4 magnetic beads. Cells were lysed in lysis buffer containing 1% Nonidet P-40 (NP-40) and analyzed for phosphorylated proteins using anti-pY.

Statistics. An unpaired two-tailed Student's *t* test was used for all the statistical analysis.

Detection of TCRβ gene rearrangement. DN thymocytes were sorted and lysed in lysis buffer containing 1% NP-40. After centrifugation, the supernatant was removed and genomic DNA was prepared from the nuclear pellet by addition of proteinase K-containing buffer. Three-fold serially diluted DNAs were used as templates. Rearrangement of the *Tcrb* gene was detected by PCR as described previously (32) using Blend Taq plus DNA polymerase (TOYOBO) and the following primers:

Vβ5-forward, 5'- CCCAGCAGATTCTCAGTCCAACAG -3'; Vβ8-forward, 5'- GCAT GGGCTGAGGCTGATCCATTA -3'; Vβ10-forward, 5'- TCCAAGGCGCTTCTCACC

TCAGTC -3'; Dβ1-forward, 5'- GCTTATCTGGTGGTTTCTTCCAGC -3'; Jβ1-reverse, 5'- GCAGAGTTCCATTTCAGAACCTAGC -3'; Vβ3-forward, 5'- ACGATTCTCTGC TGAGTGTCCTCC -3'; Jβ2-reverse, 5'- TGAGAGCTGTCTCCTACTATCGATT -3'.

Acknowledgment

We thank Dr. Harald von Boehmer for providing pTα-deficient mice; S. Itohara for providing Cδ-deficient mice; T. Yasuda and T. Kurosaki for technical instruction; H. Kawamoto for providing Tst4/dll cells; Y. Agata, Y. Yoshikai, K. Shibata, T. Ishikawa, K. Toyonaga and A. Takeuchi for discussion; K. Ogata for molecular modeling; M. Sakuma, M. Matsuda, S. Mochiduki, Y. Esaki and N. Tobe for technical assistance; Y. Nishi and H. Yamaguchi for secretary assistance; and Research Support Center, Graduate School of Medical Sciences, Kyushu University and Laboratory for Technical Support, Medical Institute of Bioreguration, Kyushu University for technical supports. This work was supported by Grant-in-Aid for Young Scientists (B) and by Kyushu University Interdisciplinary Programs in Education and Projects in Research Development (P&P) (E.I.).

The authors have no conflicting financial interests.

References

1. Wiest, D. L., Berger, M. A.,Carleton, M. (1999) Control of early thymocyte development by the pre-T cell receptor complex: A receptor without a ligand? *Semin Immunol* 11:251-62.
2. von Boehmer, H. (2005) Unique features of the pre-T-cell receptor alpha-chain: not just a surrogate. *Nat Rev Immunol* 5:571-7.
3. Irving, B. A., Alt, F. W.,Killeen, N. (1998) Thymocyte development in the absence of pre-T cell receptor extracellular immunoglobulin domains. *Science* 280:905-8.
4. Saint-Ruf, C.*, et al.* (2000) Different initiation of pre-TCR and gammadeltaTCR signalling. *Nature* 406:524-7.
5. Aifantis, I.*, et al.* (2002) A critical role for the cytoplasmic tail of pTalpha in T lymphocyte development. *Nat Immunol* 3:483-8.
6. Fehling, H. J.*, et al.* (1997) Restoration of thymopoiesis in pT alpha-/- mice by anti-CD3epsilon antibody treatment or with transgenes encoding activated Lck or tailless pT alpha. *Immunity* 6:703-14.
7. Yamasaki, S.*, et al.* (2006) Mechanistic basis of pre-T cell receptor-mediated autonomous signaling critical for thymocyte development. *Nat Immunol* 7:67-75.
8. Gibbons, D.*, et al.* (2001) The biological activity of natural and mutant pTalpha alleles. *J Exp Med* 194:695-703.
9. Haks, M. C.*, et al.* (2003) Low activation threshold as a mechanism for

ligand-independent signaling in pre-T cells. *J Immunol* 170:2853-61.

10. Palacios, E. H.,Weiss, A. (2007) Distinct roles for Syk and ZAP-70 during early thymocyte development. *J Exp Med* 204:1703-15.

11. Li, Q. J.*, et al.* (2007) miR-181a is an intrinsic modulator of T cell sensitivity and selection. *Cell* 129:147-61.

12. Kometani, K.*, et al.* (2008) Essential role of Rap signal in pre-TCR-mediated beta-selection checkpoint in alphabeta T-cell development. *Blood* 112:4565-73.

13. Trampont, P. C.*, et al.* (2010) CXCR4 acts as a costimulator during thymic beta-selection. *Nat Immunol* 11:162-70.

14. Janas, M. L.*, et al.* (2010) Thymic development beyond beta-selection requires phosphatidylinositol 3-kinase activation by CXCR4. *J Exp Med* 207:247-61.

15. Borowski, C., Li, X., Aifantis, I., Gounari, F.,von Boehmer, H. (2004) Pre-TCRalpha and TCRalpha are not interchangeable partners of TCRbeta during T lymphocyte development. *J Exp Med* 199:607-15.

16. Lacorazza, H. D., Porritt, H. E.,Nikolich-Zugich, J. (2001) Dysregulated expression of pre-Talpha reveals the opposite effects of pre-TCR at successive stages of T cell development. *J Immunol* 167:5689-96.

17. Aifantis, I., Buer, J., von Boehmer, H.,Azogui, O. (1997) Essential role of the pre-T cell receptor in allelic exclusion of the T cell receptor beta locus. *Immunity* 7:601-7.

18. Fehling, H. J., Krotkova, A., Saint-Ruf, C.,von Boehmer, H. (1995) Crucial role of the pre-T-cell receptor alpha gene in development of alpha beta but not gamma

delta T cells. *Nature* 375:795-8.

19. Panigada, M.*, et al.* (2002) Constitutive endocytosis and degradation of the pre-T cell receptor. *J Exp Med* 195:1585-97.

20. Ciofani, M.*, et al.* (2004) Obligatory role for cooperative signaling by pre-TCR and Notch during thymocyte differentiation. *J Immunol* 172:5230-9.

21. Guidos, C. J. (2006) Synergy between the pre-T cell receptor and Notch: cementing the alphabeta lineage choice. *J Exp Med* 203:2233-7.

22. von Boehmer, H.*, et al.* (1999) Pleiotropic changes controlled by the pre-T-cell receptor. *Curr Opin Immunol* 11:135-42.

23. Malissen, B.,Malissen, M. (1996) Functions of TCR and pre-TCR subunits: lessons from gene ablation. *Curr Opin Immunol* 8:383-93.

24. Michie, A. M.,Zuniga-Pflucker, J. C. (2002) Regulation of thymocyte differentiation: pre-TCR signals and beta-selection. *Semin Immunol* 14:311-23.

25. Malissen, M.*, et al.* (1992) Regulation of TCR alpha and beta gene allelic exclusion during T-cell development. *Immunol Today* 13:315-22.

26. Uematsu, Y.*, et al.* (1988) In transgenic mice the introduced functional T cell receptor beta gene prevents expression of endogenous beta genes. *Cell* 52:831-41.

27. Ji, Q., Perchellet, A.,Goverman, J. M. (2010) Viral infection triggers central nervous system autoimmunity via activation of CD8(+) T cells expressing dual TCRs. *Nat Immunol*.

28. Sakai, K.,Miyazaki, J. (1997) A transgenic mouse line that retains Cre recombinase activity in mature oocytes irrespective of the cre transgene

transmission. *Biochem Biophys Res Commun* 237:318-24.

29. Berg, L. J.,Davis, M. M. (1989) T-cell development in T cell receptor alphabeta transgenic mice. *Semin Immunol* 1:105-16.

30. Itohara, S.*, et al.* (1993) T cell receptor delta gene mutant mice: independent generation of alpha beta T cells and programmed rearrangements of gamma delta TCR genes. *Cell* 72:337-48.

31. Masuda, K.*, et al.* (2005) Thymic anlage is colonized by progenitors restricted to T, NK, and dendritic cell lineages. *J Immunol* 174:2525-32.

32. Agata, Y.*, et al.* (2007) Regulation of T cell receptor beta gene rearrangements and allelic exclusion by the helix-loop-helix protein, E47. *Immunity* 27:871-84.

Figure legends

Figure 1. Generation of 'charge-less' pTα knock-in mice.

(A) Locations of point mutations in the pTα mutant. The four charged residues in the extracellular domain of pTα were replaced by alanine.

(B) Genomic *Ptcra* structure and targeting constructs. Each mutation located in exon2 and exon3 was indicated by asterisks. Open triangles, *loxP* sites. Arrows, the primers used for genomic PCR.

(C) Genomic PCR. Genomic DNAs from WT ($pT\alpha^{+/+}$), $pT\alpha^{4A/+}$, and $pT\alpha^{4A/4A}$ mice were amplified with primers that cross over *loxP* sites, indicated as arrows in (B).

(D) mRNA expression of the charge-less pTα mutant. $CD4^{-}CD8^{-}$ (DN) thymocytes from $pT\alpha^{+/+}$, $pT\alpha^{4A/+}$, $pT\alpha^{4A/4A}$, and $pT\alpha^{-/-}$ mice were analyzed by real-time RT-PCR using common (pan-pTα), $pT\alpha^{WT}$- and $pT\alpha^{4A}$-specific primers as described in Materials and Methods. Data are represented as mRNA levels relative to that of β-actin. Each value is the mean ± s.d. for triplicate assays.

(E) Surface staining of pre-TCR complex. DN thymocytes from $pT\alpha^{+/+}$, $pT\alpha^{4A/4A}$, and $pT\alpha^{-/-}$ mice were stained with anti-pTα, anti-IgG_1-biotin, and streptavidin-APC (upper panels) or with anti-TCRβ-APC (lower panels), as described in the Materials and Methods section. Non-labeled mouse IgG_1 mAb and APC-labeled hamster IgG_2 were used as isotype controls for anti-pTα and anti-TCRβ, respectively (thin histograms).

Figure 2. DN-to-DP thymocyte development was impaired in $pT\alpha^{4A/4A}$ mice.

(A–B) Thymocyte numbers. Thymocytes from four-week-old mice were analyzed for the

absolute number of total thymocytes (A), $CD4^{-}CD8^{-}$ population (DN) and $CD4^{+}CD8^{+}$ population (DP) (B). Each symbol represents an individual mouse. **, $p < 0.01$.

(C) Flow cytometric profiles of whole thymocytes from WT ($pT\alpha^{+/+}$), $pT\alpha^{4A/4A}$ and $pT\alpha^{-/-}$ mice. The percentages of thymocytes in each quadrant are shown. Data are representative of four independent experiments.

(D) *In vitro* thymocyte differentiation. DN cells negatively sorted by anti-CD8 and anti-CD4 magnetic beads were cultured on Tst-4/DLL1 stromal cells. At day 0 (upper panels) and day 2 (lower panels), cells were analyzed for DN-to-DP transition. The percentage of DP population is shown. Data are representative of three independent experiments.

(E) Thymocytes were analyzed for the expression of CD25 and CD44 within the $CD4^{-}CD8^{-}$ (DN)-gated population, and the percentages of $CD44^{-}CD25^{+}$ (DN3) cells among the whole thymocytes were plotted as in (A). Each symbol represents an individual four-week-old mouse. **, $p < 0.01$.

(F) Thymocytes were stained with anti-TCRδ and anti-CD3ε antibodies, and the percentages of γδ T cells in the whole thymocytes were plotted as in (E). **, $p < 0.01$.

(G) Thymic cellularity of $pT\alpha^{4A/4A} \times TCR\delta^{-/-}$ mice. Total thymocyte numbers and percentages of DN3 population were also shown. Data are representative of three independent experiments.

Figure 3. Impaired β-selection and pre-TCR proximal signaling in $pT\alpha^{4A/4A}$ mice.

(A) BrdU incorporation into thymocytes. WT ($pT\alpha^{+/+}$) and $pT\alpha^{4A/4A}$ mice were injected

intraperitoneally with BrdU. At 4 h after injection, thymocytes were stained with anti-BrdU, anti-CD4, anti-CD8, anti-CD44, and anti-CD25 mAbs. Percentage of BrdU-positive cells within each population are shown. Data are representative of three independent experiments.

(B) Competitive repopulation assay. BM cells from Ly5.1^{+} WT mice and Ly5.2^{+} pT$\alpha^{4A/4A}$ mice were mixed in a ratio of 1:1 and injected into irradiated Rag1$^{-/-}$ mice. Reconstituted thymi and spleens were analyzed 4 weeks later for Ly5.1^{+} (WT) and Ly5.2^{+} (pT$\alpha^{4A/4A}$) cells. Each sample of mixed BM cells was injected into at least five recipient mice of matched sex and age, and representative data of similar results are shown.

(C) Pre-TCR-induced phosphorylation. Freshly-isolated DN thymocytes from Rag1$^{-/-}$, pT$\alpha^{+/+}$, pT$\alpha^{4A/4A}$ and pT$\alpha^{-/-}$ mice were detected by Western blot analysis with anti-phospho tyrosine Ab (pY). The membrane was also blotted with anti-CD3ε as a loading control. Data are representative of four independent experiments.

Figure 4. Break of allelic exclusion in pT$\alpha^{4A/4A}$ mice.

(A) Schematic diagram of the TCRβ locus and the location of the primers used for detection of rearranged TCRβ genes. Gray box, Pseudo gene.

(B) Rearrangement of *Tcrb* allele. Genomic DNA purified from DN thymocytes was analyzed for TCRβ rearrangement using the primers described in (A). Transgenic Vβ3-Jβ2 (TCRβ^{Tg}), pTα^{WT} and pTα^{4A} alleles were also detected as a control for the amount of input DNA as well as for genotypes. Data are representative of three independent experiments.

Figure 5. Emergence of dual TCRβ expresser in pTα$^{4A/4A}$ mice.

(A) Detection of T cells expressing dual TCRβ on the surface. SP thymocytes (upper panel) and splenic T cells (lower panel) from TCRβ Tg mice were stained with PE-labeled anti-Vβ3 together with a mixture of FITC-labeled anti-Vβ2, 4, 5.1/5.2, 6, 7, 8.1/8.2, 8.3, 9, 10, 11, 12, 13, 14 and 17a ($V\beta_{endo}$).

(B) Frequency of dual TCRβ expresser. Thymocytes (left panel) and splenic T cells (right panel) were analyzed for the percentage of dual expresser ($V\beta3^+V\beta_{endo}^+$) in $V\beta3^+$ population. Data are means ± s.d. of three independent mice. *, $p < 0.05$.

(C) Frequency of dual TCRβ expresser in non-TCR Tg mice. SP thycmoytes (left panel) and splenic T cells (right panel) from WT (pTα$^{+/+}$), pTα$^{4A/+}$ and pTα$^{4A/4A}$ mice were stained with PE-labeled anti-Vβ3 or Vβ5 together with a mixture of FITC-labeled mAbs specific for the other Vβs. Percentage of $V\beta3^+V\beta_{endo}^+$ and $V\beta5^+V\beta_{endo}^+$ T cells was shown, respectively. Data are means ± s.d. of three independent mice. *, $p < 0.05$.

Data are representative of three independent experiments.

Figure 6. Altered distribution of TCRVβ in pTα$^{4A/4A}$ mice

(A) $CD4^+CD8^-$ (left panel) and $CD4^-CD8^+$ (right panel) thymocytes from WT, pTα$^{4A/+}$ and pTα$^{4A/4A}$ mice were stained with anti-Vβs and analyzed by flow cytometry.

(B) Distribution of Vβs in splenic $CD4^+$ T cells (left panel) and $CD8^+$ T cells (right panel) from WT, pTα$^{4A/+}$ and pTα$^{4A/4A}$ mice were analyzed as in (A). Data are means ± s.d. for at least three independent mice. Representative results from two independent experiments

with similar results are shown. *, $p < 0.05$. **, $p < 0.01$.

Figure 1

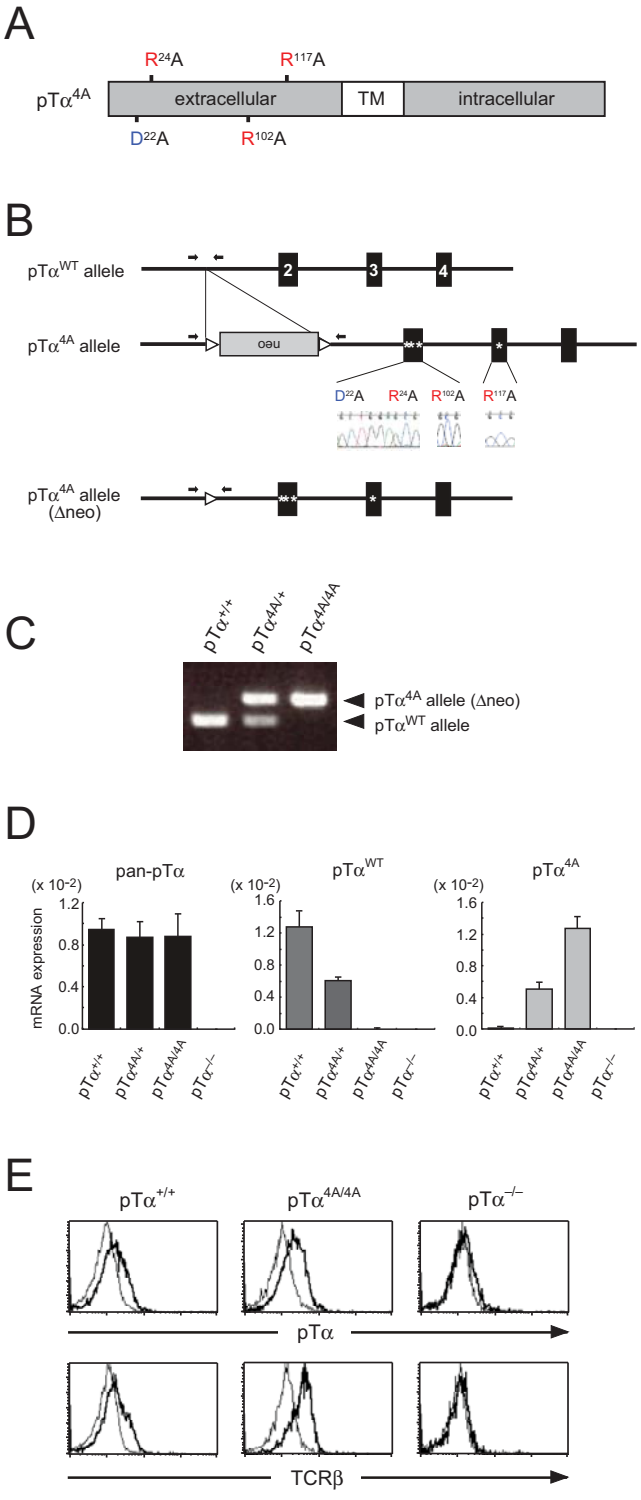
A
R24A
R117A
pTα4A
extracellular
TM
intracellular
D22A
R102A
B
pTαWT allele
2
3
4
pTα4A allele
oeu
D22A
R24A
R102A
R117A
pTα4A allele
(Δneo)
C
pTα+/+
pTα4A/+
pTα4A/4A
pTα4A allele (Δneo)
pTαWT allele
D
pan-pTα
pTαWT
pTα4A
(x 10-2)
mRNA expression
1.2
0.8
0.4
0.0
1.6
pTα+/+
pTα4A/+
pTα4A/4A
pTα−/−
E
pTα+/+
pTα4A/4A
pTα−/−
pTα
TCRβ

Figure 2

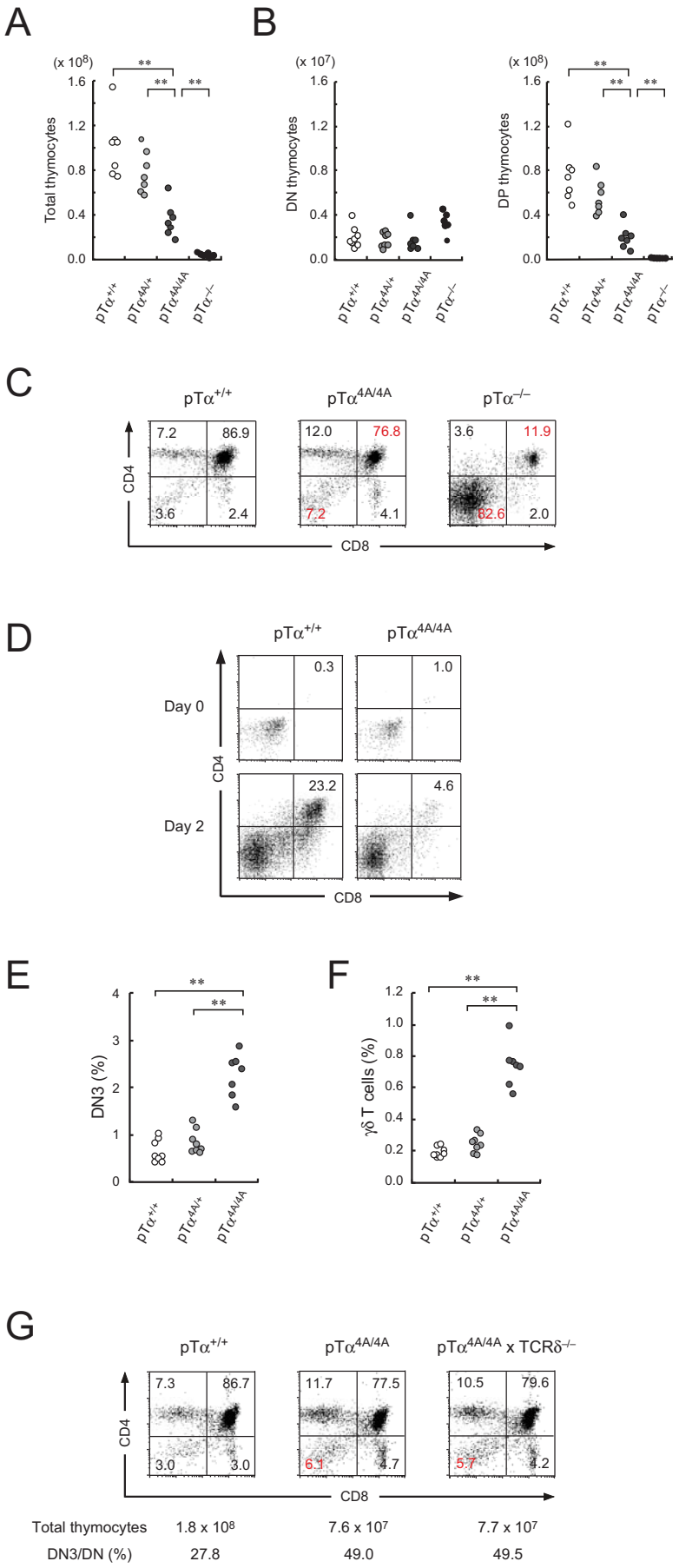
A
B
C
D
E
F
G
Total thymocytes
DN thymocytes
DP thymocytes
(x 10^8)
(x 10^7)
**
pTα+/+
pTα4A/+
pTα4A/4A
pTα−/−
CD4
CD8
Day 0
Day 2
DN3 (%)
γδ T cells (%)
pTα4A/4A x TCRδ−/−
Total thymocytes 1.8 x 10^8 7.6 x 10^7 7.7 x 10^7
DN3/DN (%) 27.8 49.0 49.5

Figure 3

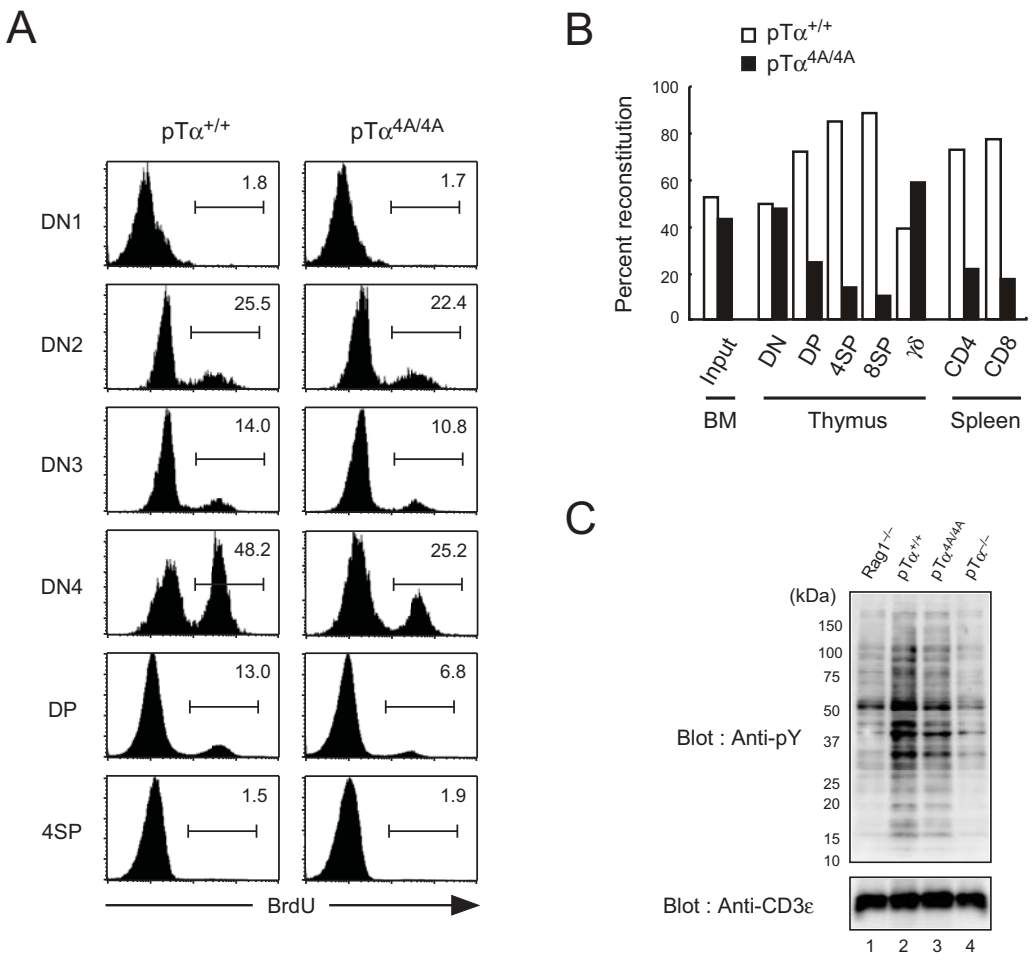
A
pTα+/+
pTα4A/4A
DN1
DN2
DN3
DN4
DP
4SP
1.8
1.7
25.5
22.4
14.0
10.8
48.2
25.2
13.0
6.8
1.5
1.9
BrdU
B
pTα+/+
pTα4A/4A
Percent reconstitution
100
80
60
40
20
0
Input
DN
DP
4SP
8SP
γδ
CD4
CD8
BM
Thymus
Spleen
C
Rag1-/-
pTα+/+
pTα4A/4A
pTα-/-
(kDa)
150
100
75
50
37
25
20
15
10
Blot : Anti-pY
Blot : Anti-CD3ε
1 2 3 4

Figure 4

A

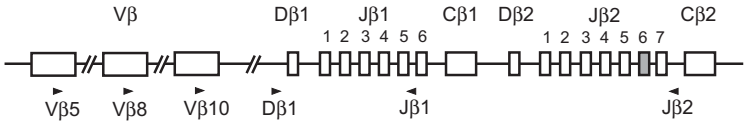
Vβ
Dβ1
Jβ1
Cβ1
Dβ2
Jβ2
Cβ2
1 2 3 4 5 6
1 2 3 4 5 6 7
Vβ5
Vβ8
Vβ10
Dβ1
Jβ1
Jβ2

B

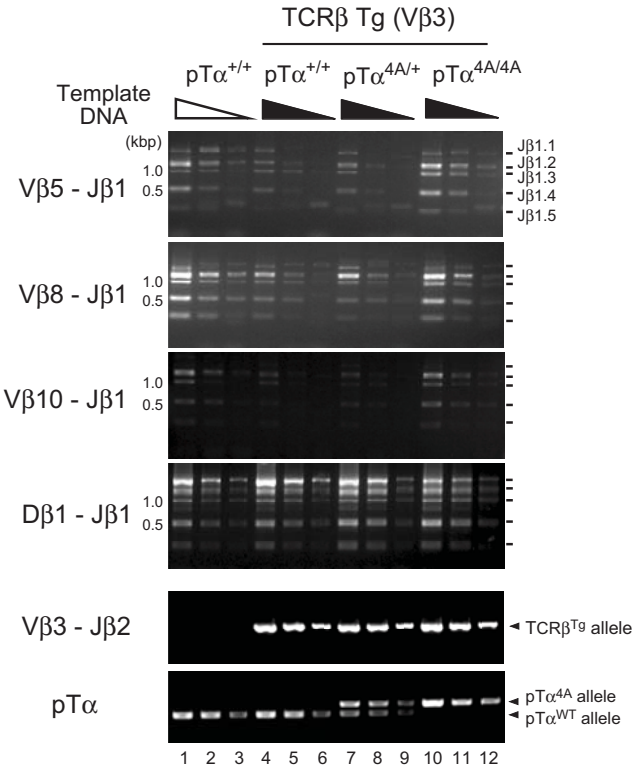
TCRβ Tg (Vβ3)
pTα+/+
pTα+/+
pTα4A/+
pTα4A/4A
Template DNA
(kbp)
Vβ5 - Jβ1
Vβ8 - Jβ1
Vβ10 - Jβ1
Dβ1 - Jβ1
1.0
0.5
Jβ1.1
Jβ1.2
Jβ1.3
Jβ1.4
Jβ1.5
Vβ3 - Jβ2
TCRβTg allele
pTα
pTα4A allele
pTαWT allele
1 2 3 4 5 6 7 8 9 10 11 12

Figure 5

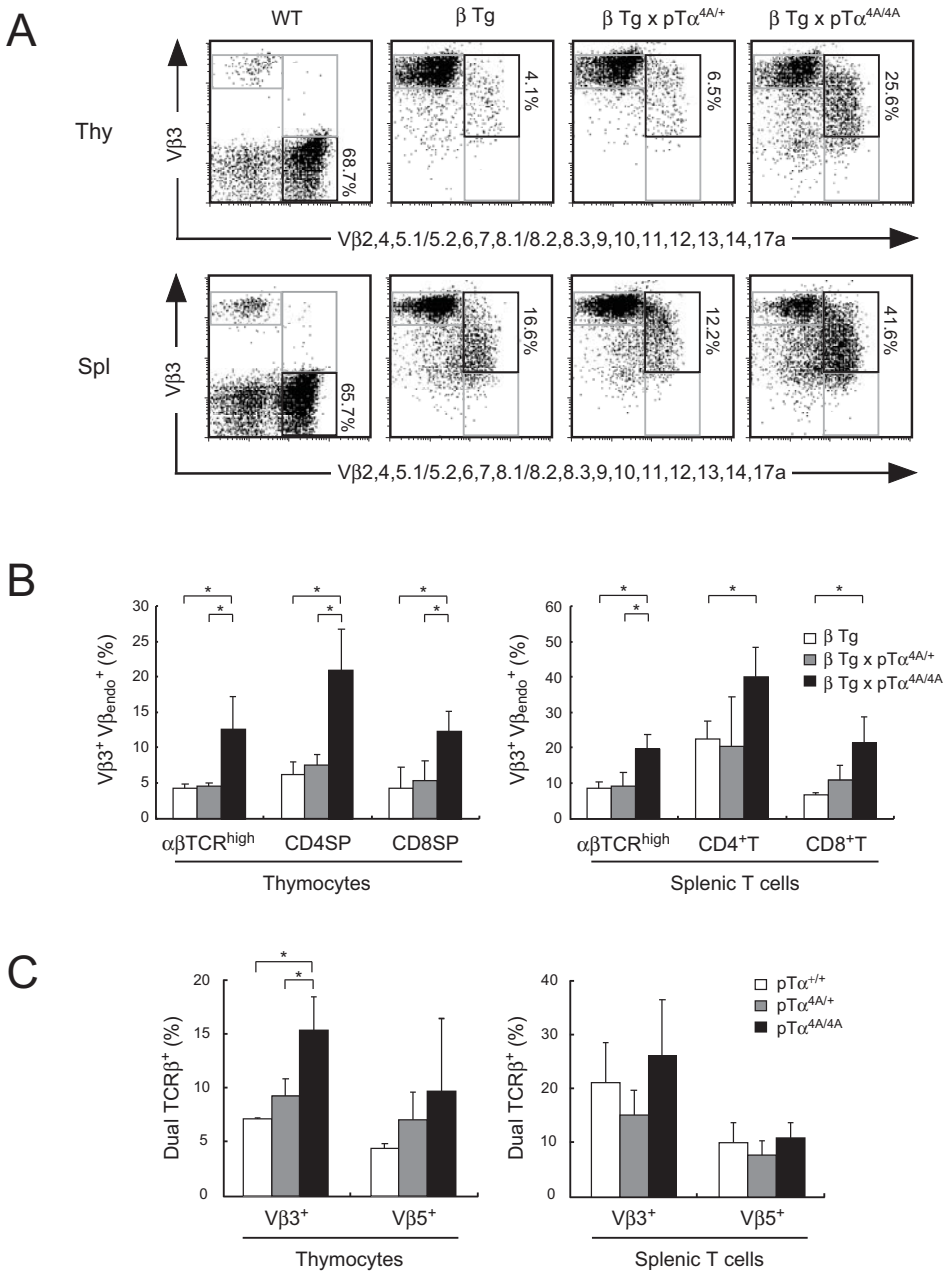
A
WT
β Tg
β Tg x pTα4A/+
β Tg x pTα4A/4A
Thy
Spl
Vβ3
68.7%
4.1%
6.5%
25.6%
65.7%
16.6%
12.2%
41.6%
Vβ2,4,5.1/5.2,6,7,8.1/8.2,8.3,9,10,11,12,13,14,17a
B
Vβ3+ Vβendo+ (%)
αβTCRhigh
CD4SP
CD8SP
Thymocytes
CD4+T
CD8+T
Splenic T cells
β Tg
β Tg x pTα4A/+
β Tg x pTα4A/4A
C
Dual TCRβ+ (%)
Vβ3+
Vβ5+
pTα+/+
pTα4A/+
pTα4A/4A

Figure 6

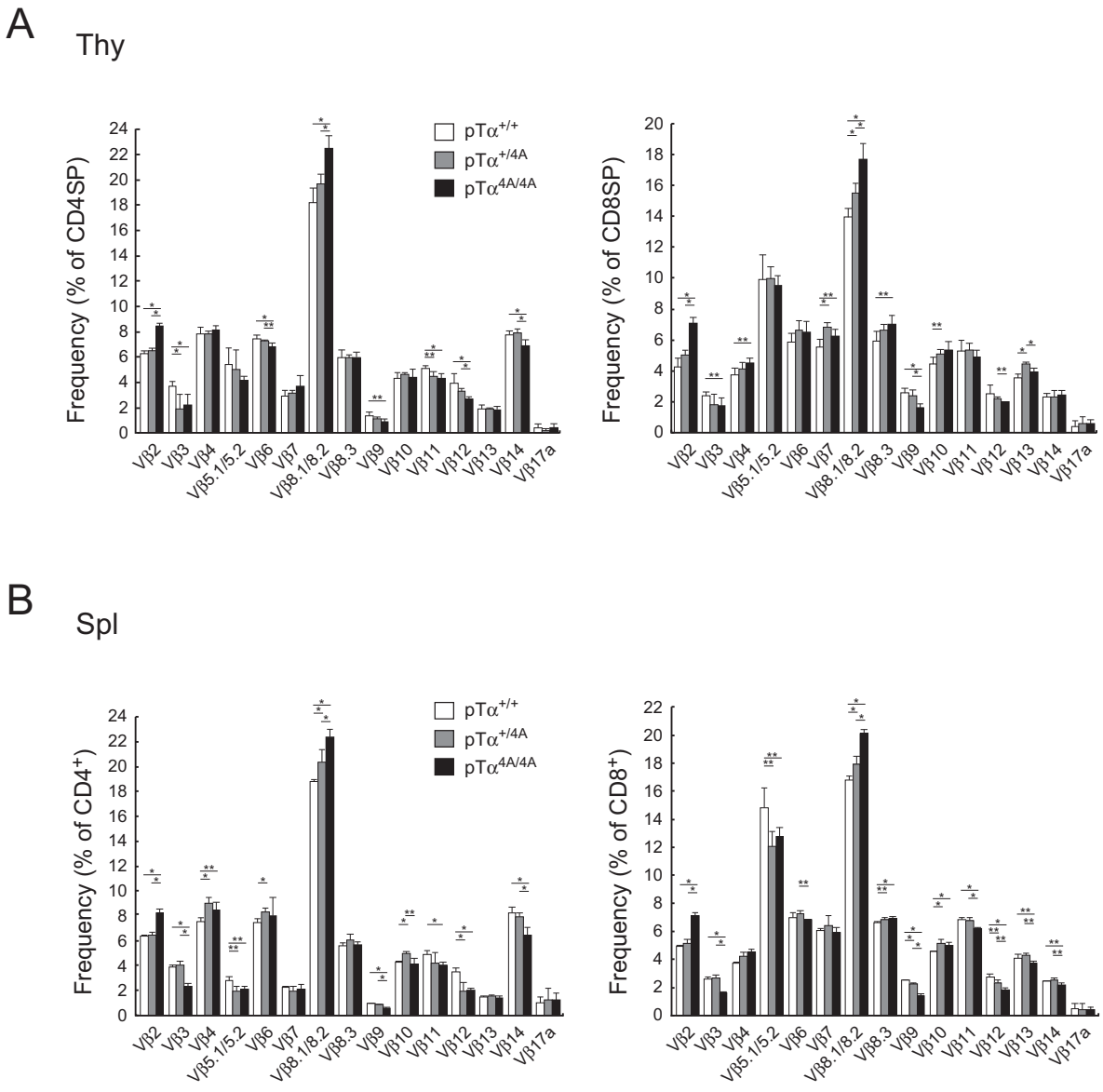
A
Thy
Frequency (% of CD4SP)
Frequency (% of CD8SP)
pTα+/+
pTα+/4A
pTα4A/4A
Vβ2
Vβ3
Vβ4
Vβ5.1/5.2
Vβ6
Vβ7
Vβ8.1/8.2
Vβ8.3
Vβ9
Vβ10
Vβ11
Vβ12
Vβ13
Vβ14
Vβ17a
B
Spl
Frequency (% of CD4+)
Frequency (% of CD8+)